Slaved diffusion in phospholipid bilayers

Liangfang Zhang and Steve Granick*

Materials Research Laboratory and Department of Chemical and Biomolecular Engineering, University of Illinois, Urbana, IL 61801

Edited by Nicholas J. Turro, Columbia University, New York, NY, and approved May 19, 2005 (received for review April 4, 2005)

The translational diffusion of phospholipids in supported fluid bilayers splits into two populations when polyelectrolytes adsorb at incomplete surface coverage. Spatially resolved measurements using fluorescence correlation spectroscopy show that a slow mode, whose magnitude scales inversely with the degree of polymerization of the adsorbate, coexists with a fast mode characteristic of naked lipid diffusion. Inner and outer leaflets of the bilayer are affected nearly equally. Mobility may vary from spot to spot on the membrane surface, despite the lipid composition being the same. This work offers a mechanism to explain how nanosized domains with reduced mobility arise in lipid membranes.

adsorption | fluorescence correlation | mobility

Phospholipid bilayers supported on planar substrates (1, 2) and in free-standing vesicles (3, 4) are fundamental not only in biology but also in applied problems such as their use as biosensors and nanoreactors. We are interested here in what determines the lateral mobility of the individual molecules that comprise these fluid yet two-dimensional systems, a problem that is fundamental to their function. Important prior studies considered how lipid diffusion depends on chemical composition and phase state of the bilayer (5–7) but dealt with naked bilayers (no adsorption). Others studied how mixtures of phospholipids partition spatially after encounter with an adsorbate (8) but did not address mobility of these lipids. Binding-induced mobility changes also have been considered (9, 10). To the best of our knowledge, all prior studies of lipid mobility have considered area-averaged quantities, leaving open the possibility that the area-average might mask an interesting distribution.

Here, we show that adsorption of a flexible macromolecule produces dynamical heterogeneity even in bilayers comprised of one single type of phospholipid. We consider bilayers supported on a planar substrate because they present the advantage of a well-defined geometry while retaining lipid fluidity similar to that in freestanding vesicles (11).

Materials and Methods

The measurement method was fluorescence correlation spectroscopy (12). Two-photon excitation at the diffraction-limited focus of a laser beam enabled measurements that were spatially resolved. Near-infrared light from a femtosecond Ti:Sapphire laser (800 nm, 82 MHz, pulse width $\approx$100 fsec) was focused onto the sample through a water immersion objective lens (Zeiss Axiovert 135 TV, $\times$63, numerical aperture 1.2). Fluorescence was excited only at the focus, giving an excitation spot whose diffraction-limited diameter was $\approx$0.35 μm. Fluorescence was collected through the same objective and detected by a single photon counting module (Hamamatsu, Middlesex, NJ). The 10-ppm concentration of fluorescent label was selected such that on average one sole fluorescent molecule resided within the area sampled. In deducing the diffusion coefficients presented below, each is the average of 10–20 experiments performed at different locations on the surface, and the error bars show the standard deviation (SD).

The phospholipid 1,2-dilauroyl-*sn*-glycero-3-phosphocholine (DLPC; Avanti Polar Lipids) was selected because its gel-to-fluid phase transition of -1°C was well below the experimental temperature, 23°C. Into DLPC we doped at 10 ppm molar concentration 1,2-dimyristoyl-*sn*-glycero-3-phosphoethanolamine (DMPE), with polar head group labeled by rhodamine B. By using known protocols based on the fusion of single unilamellar vesicles (13, 14), supported bilayers of the mixture were prepared on hydrophilic quartz, then rinsed with copious amounts of PBS buffer (pH 6.0) to remove unfused vesicles. In subsequent adsorption of polymers (Polymer Source, Quebec), when wishing to present a negatively charged object to the bilayer we used poly(methacrylic acid). When wishing to present a positively charged polymer, we used fully quaternized poly-4-vinylpyridine (QPVP) prepared by us from parent polyvinylpyridine by reaction with an excess of ethyl bromide (15). To calibrate the surface coverage after adsorption, parallel measurements were made using Fourier transform infrared spectroscopy in the mode of attenuated total reflection of polymer adsorbed to DLPC bilayers supported on silicon substrates; the methods are described in ref. 16. Surface coverage was controlled by allowing adsorption for a limited time after which the bilayer was "starved" of polymer by replacing the polymer solution with pure buffer, and the range of surface coverage was kept sufficiently low that the polymer was expected to adsorb flattened against the membrane as a "pancake" (16). All measurements were made in PBS buffer (10 mM, pH 6.0).

Results

The curious data that motivated this study are summarized in Fig. 1. Depending on where the laser was focused, the rate of fluorescence fluctuation switched between two states; it varied from spot to spot on the bilayer in a bimodal way. In Fig. 1, the intensity–intensity fluorescence autocorrelation function computed from the observed fluctuations is plotted against logarithmic time lag after the cationic polymer, QPVP, was allowed to adsorb to partial surface coverage (see Fig. 1 legend). Control experiments of diffusion in the naked bilayer (no polymer adsorbed) are included in Fig. 2. They gave a single autocorrelation function with nearly the same time scale as the fast process in the presence of adsorbate (see below).

The physical meaning of the autocorrelation function is to quantify the time for Fickian diffusion through the spot illuminated by the focused laser beam; then, the translational diffusion coefficient D scales as the square of its linear dimension, divided by the time at which the autocorrelation function decayed to a given value. Quantitative elaboration of this idea, standard in fluorescence correlation spectroscopy, also takes into account the Gaussian shape of the spot illuminated by the laser beam (17). Note that additional scatter enters the fluorescence autocorrelation curves at the shortest time delays, mainly because of fluorescence triplet noise; this effect does not influence analysis of the translational diffusion processes that occur on the millisecond to hundreds of milliseconds time range. The lines through the data in Fig. 1 are fits with one fitting parameter, the diffusion coefficient. Although the quality of fit is excellent, the slower mode in Fig. 1 can be described equally well by allowing

This paper was submitted directly (Track II) to the PNAS office.

Abbreviations: DLPC, 1,2-dilauroyl-*sn*-glycero-3-phosphocholine; QPVP, quaternized poly-4-vinylpyridine.

*To whom correspondence should be addressed. E-mail: sgranick@uiuc.edu.

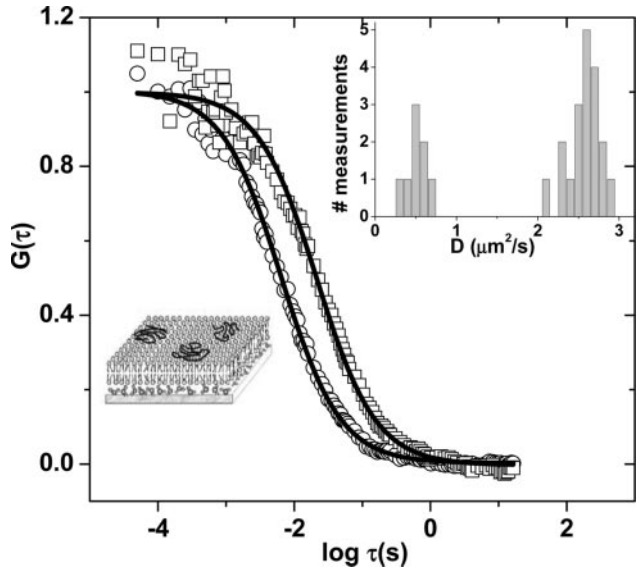

Fig. 1. Fluorescence autocorrelation function $G(\tau)$ plotted as a function of logarithmic time lag τ for DLPC supported lipid bilayer carrying adsorbed QPVP at the fractional surface coverage of 20%. The QPVP was 100% quaternized with weight-average molar mass 81,500 g·mol^{-1}. Note that fast and slow diffusion modes coexist depending on where the interrogatory laser spot was focused. (*Inset*) Histogram of diffusion coefficients obtained from ≈30 different measurements on a number of samples. The mean D of the slow mode is 0.50 μm^2·sec^{-1} with SD of 0.12, whereas the mean D of the fast mode is 2.62 μm^2·sec^{-1} with SD of 0.18.

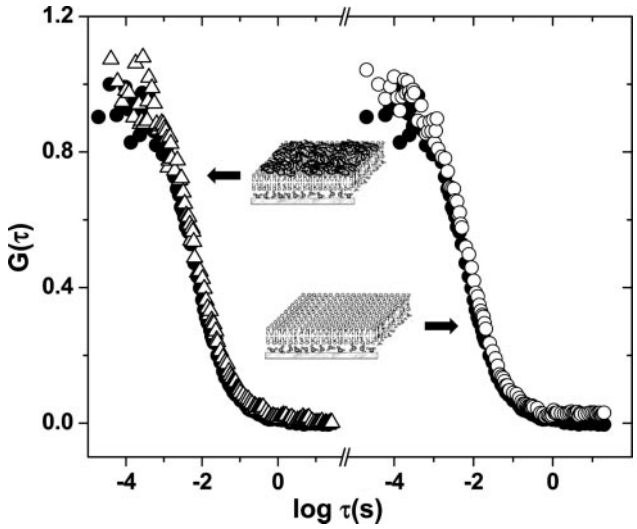

Fig. 2. The time scale of lipid diffusion, measured by the fluorescence autocorrelation function $G(\tau)$ plotted as a function of time lag τ, is compared in situations indicated by the schematic cartoons. The cartoon on the left shows lipids diffusing in the naked DLPC bilayer (●) and after saturated adsorption by QPVP (△). Saturated adsorption was 0.95 mg·m^{-2}. The cartoon on the right shows lipids diffusing in the naked DLPC bilayer with fluorescence from both the inner and the outer leaflets of these bilayers (●) and for diffusion solely in the bottom leaflet of the naked bilayer (○).

up to 20% contribution from the faster mode, which is reasonable physically.

This finding would be trivial if it stemmed from some kind of specific binding of lipid to the adsorbed polymer, but this possibility was ruled out when it emerged that the slower mode disappeared when the bilayer was saturated with adsorbed polymer. The data are included in Fig. 2. Quantitative analysis shows that the implied diffusion coefficient when the bilayers was saturated with adsorbed polymer was only 8% less than that of naked lipid, i.e., nearly the same within the experimental uncertainty. Making the reasonable assumption of an Arrhenius dependence of D, and taking 8% as the upper limit of the actual difference, this result implies that the adsorption energy to polymer was ≤80 kJ/mol. With a reasonable assumption of the area occupied by the polymer, this value amounts to ≤0.08 k_BT per lipid at this temperature. (Here k_B is the Boltzmann constant and T is the absolute temperature.) The uninteresting possibility of specific binding was thus eliminated.

A more interesting hypothesis was that the slower mode, observed when the surface coverage by polymer was incomplete, represented lipids diffusing coherently with adsorbed polymer. How to test this idea? First, we tested robustness of the effect by varying the surface coverage of adsorbed polymer. In Fig. 3, the faster and slower diffusion coefficients are plotted as a function of surface coverage of adsorbate, the surface coverage ranging up to 40% of saturated coverage. One sees that both the fast and slow modes remained constant within experimental uncertainty but that as the surface coverage increased, their relative intensities changed linearly, as should happen physically if the slow mode grew at the expense of the fast mode. Because the adsorbed QPVP macromolecules carried a positive charge at every segment, it appears that electrostatic repulsion prevented them from overlapping significantly, thus enabling them to diffuse independently up to these relatively high levels of surface coverage without showing any dependence on the surface coverage. Fig. 3 includes a histogram of diffusion coefficients measured in many such experiments.

A second control experiment investigated the scenario in which diffusion of the fluorescent-labeled lipid slowed for the trivial reason that it bound electrostatically to the adsorbed polymer. To test this hypothesis, the adsorbate was switched to be anionic rather than cationic while retaining the same fluorescent-labeled lipid, which was anionic. When poly(methacrylic acid) was allowed to adsorb, the same bimodal split was observed as for QPVP in Figs. 1 and 3, thus ruling out this possibility. A quantitative analysis of this result is discussed below in connection with Fig. 4.

Third, we considered the possibility that lipids in the top and bottom leaflets of the solid-supported bilayers might diffuse at different rates. Control experiments were performed in which fluorescence in the top leaflet was quenched by adding iodide ions to the solution. Iodide is an efficient quencher of fluorescence by means of the heavy-ion effect yet does not penetrate phospholipid bilayers (18). In Fig. 2, it is obvious that the fluorescence autocorrelation function in phosphate buffer solution with 50 mM KI nearly overlaps with data taken in the absence of quencher. Although there is a slight difference on the order of 10%, the main point is to show that lipid diffusion on the two sides of the supported bilayer was so strongly coupled as to be nearly the same. Possible reasons for such coupling have been considered theoretically (19).

Next, we used a method described in ref. 16 to eliminate the possible objection that the positively charged adsorbate burrowed beneath the bilayer to bind with the quartz substrate, which was negatively charged.

Having, with these control experiments, ruled out trivial explanations, the influence of polymer molar mass was investigated. Always a fast and a slow mode were observed. The higher the molar mass, the slower the diffusion. In Fig. 4, the diffusion coefficient (D) inferred from the slow mode is plotted on log–log scales against degree of polymerization of the polymer (N); the chain length varies by nearly an order of magnitude and the comparison is made at fixed surface coverage, 20% of saturated

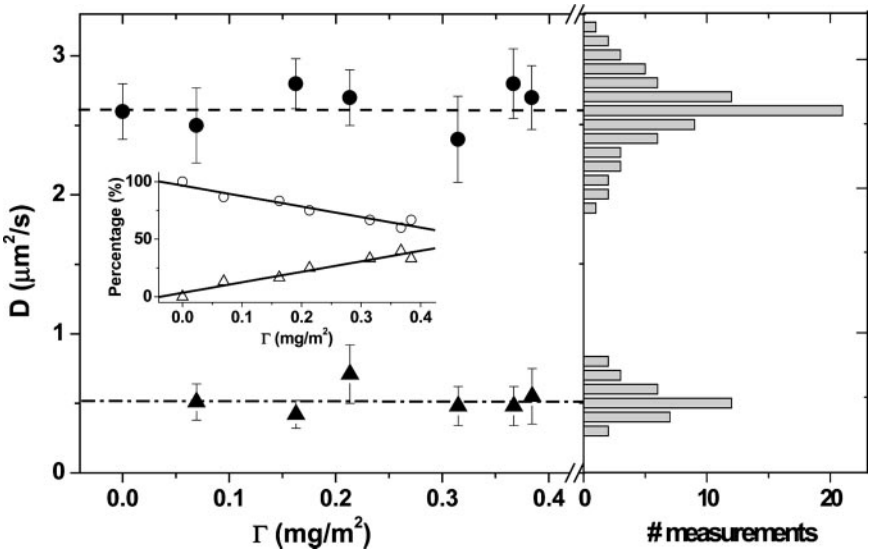

Fig. 3. Surface coverage dependence when surface coverage was <50%. (*Left*) Diffusion coefficients of the fast and slow modes of lipid motion, plotted against surface coverage for the same system as in Fig. 1. (Error bars show SD.) *Inset* shows the relative amplitudes of the fast mode (○) and slow mode (△) plotted against surface coverage. (*Right*) Histograms of fast and slow diffusion coefficients obtained from ≈100 different measurements on a number of samples.

adsorption. The plot shows a clear empirical power law relationship, $D \propto N^{-1}$. Considering that the datum concerning adsorbed poly(methacrylic acid) (opposite charge to QPVP) falls on the same line as for QPVP, we conclude that this relation holds regardless of the charge of the adsorbed polymer. Unfortunately, for technical reasons involving the difficulty of labeling with suitable fluorescent dyes, we are not able yet to measure diffusion of these polymer adsorbates directly. However, the pioneering experiments of Maier and Rädler (20, 21), which measured diffusion of adsorbed DNA, show precisely this same dependence on the number of base pairs N. The admittedly large extrapolation from the high molar masses in the DNA study (on the order of 3×10^7) to the much smaller molar masses studied here predicts that D (for $n = 750$) $= 0.5$ μm^2/sec. This extrapolation is consistent with the data in Fig. 4. It seems that diffusion of lipids in the bilayer was slaved to the molecules on top.

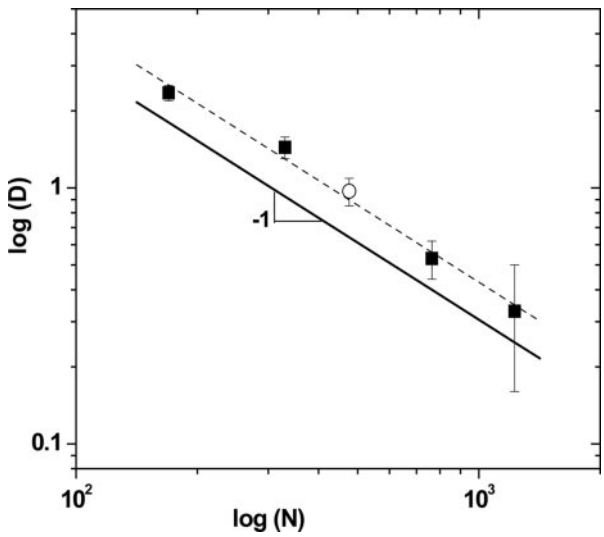

Fig. 4. Dependence on polymer degree of polymerization when surface coverage was <50%. The slow-mode diffusion coefficient is plotted against degree of polymerization of the adsorbed polymer on log–log scales; the reference solid line has slope of −1. The comparison is made at 20% of saturated surface coverage. The fully quaternized QPVP samples were prepared from parent polyvinylpyrodine samples with molar masses M_w = 18,100, 34,200, 81,500, and 130,000 g·mol^{-1} (ratio of weight-average to number-average molar mass M_w/M_n = 1.11, 1.23, 1.18, and 1.24, respectively) (■). The adsorbed poly(methacrylic acid) had M_w = 40,000 g·mol^{-1} (M_w/M_n = 1.05) (○). These data extrapolate as $N \rightarrow 150$ to D characteristic of the naked lipid, implying that the slow mode disappears below a critical adsorbate size, a projected area of ≈80 lipid head groups.

Discussion

The most plausible interpretation of the influence of polymer molar mass and the coexistence of fast and slow diffusion in the same system is that polymer adsorption created nanodomains of lipid whose mobility was determined by the occluded area of the adsorbed polymer. The multivalency of these nanodomains, the multiple potential adsorption sites to which the lipid can bind, localizes lipids because the tendency to adsorb at any individual spot is amplified by the large number of potential binding sites. The data in Fig. 4 show that as $N \rightarrow 150$, D extrapolates to that characteristic of the naked lipid, implying that the slow mode disappears below a critical adsorbate size, the projected area of ≈80 lipid head groups. This result also explains why the slow mode disappears at saturated surface coverage: then there no longer exist localized multivalent binding sites. When surface coverage by the adsorbed polymers saturated, the multivalency of the discrete nanodomain situation disappeared. The ensuing homogeneous environment possessed a local binding energy only negligibly different from that of the naked bilayer.

Exploring this argument, we note that the size of these molecular-sized domains can tentatively be estimated from R_g, the radius of gyration of the two-dimensional adsorbed polymer. For adsorbed QPVP chains, the persistence length can be estimated as 1.4 nm and the monomer length can be set as 0.26 nm. This estimate implies $R_g \approx 4$ and 9 nm for the molar masses 18,100 and 81,500 g·mol^{-1}, respectively, in turn implying surface areas $A \approx 50$ and 250 nm^2, respectively. To put these results into perspective, for those lipids trapped in such nanodomains, these arguments suggest that collective diffusion as a unit replaced the independent diffusion of individual lipid molecules. The translational mobility of a particle embedded in biological membranes

has been considered theoretically (22). These experiments show that lipid mobility is itself modified.

In summary, these measurements show how adsorption of objects of variable size modifies the mobility of lipids underneath the adsorbed object. The dependence on molar mass of the adsorbed molecule displays the same phenomenology as the diffusion of that same adsorbed macromolecule; diffusion of the lipid appears to be slaved to it. Much prior work has taken the approach of considering the area-average mobility in membranes, but we have shown here that this approach is not always a good one; mobility may vary from spot to spot on the membrane surface, despite the lipid composition being the same.

This work offers a mechanism of domain formation in lipid membranes. Traditionally, one thinks of situations where the spatial composition differs in the case of multiple lipid components, owing either to limited miscibility or the presence of stiffness-altering components such as cholesterol (23). The role of ensuing "rafts" in particular sees extensive discussion (24). In the present simpler system, this work shows that the process of polymer adsorption accomplishes this same function. The mechanism is possibly related to the known fact that adsorption modifies the local bending rigidity and the local spontaneous radius of curvature (25). This finding provides a perspective from which to interpret the physical heterogeneity that has been observed repeatedly over the years in more complicated systems involving multiple lipid components (8). By rational extension, there are possible implications for understanding dynamical events that depend on lipid mobility. If this effect generalizes to cellular environments, adsorption of peripheral membrane proteins to the outside of a cell may affect not just the mobility of the lipids underneath but also of those on the other leaflet, on the cytosolic side (and conversely). Similarly, one can imagine that it may have bearing on protein distributions in the membrane and in this manner influence docking, formation of synapses, and other membrane-mediated functions.

We thank Steven Boxer, Gerard Wong, Kenneth Schweizer, and Howard Stone for helpful discussion. This work was supported by U.S. Department of Energy, Division of Materials Science Award No. DEFG02-02ER46019 through the Frederick Seitz Materials Research Laboratory (University of Illinois at Urbana-Champaign). The fluorescence correlation spectroscopy equipment was supported under Award DEFG02-02ER46019. Some support also was provided by National Science Foundation Nanoscience Engineering Initiative NSF-DMR-0071761.

1. Sackmann, E. (1996) *Science* **271,** 43–48.
2. Boxer, S. G. (2000) *Curr. Opin. Chem. Biol.* **4,** 704–709.
3. Bolinger, P.-Y., Stamous, D. & Vogel, H. (2004) *J. Am. Chem. Soc.* **126,** 8594–8595.
4. Boukobza, E., Sonnenfeld, A. & Haran, G. (2001) *J. Phys. Chem. B* **105,** 12165–12170.
5. Ratto, T. V. & Longo, M. L. (2002) *Biophys. J.* **83,** 3380–3392.
6. Wagner, M. L. & Tamm, L. K. (2001) *Biophys. J.* **81,** 266–275.
7. Filippov, A., Orädd, G. & Lindblom, G. (2004) *Biophys. J.* **86,** 891–896.
8. Raudino, A. & Castelli, F. (1997) *Macromolecules* **30,** 2495–2502.
9. Yuan, Y., Velev, O. D. & Lenhoff, A. M. (2003) *Langmuir* **19,** 3705–3711.
10. Yamazaki, V., Sirenko, O., Schafer, R. J. & Groves, J. T. (2005) *J. Am. Chem. Soc.* **127,** 2826–2827.
11. Sonnleitner, A., Schütz, G. J. & Schmidt, T. (1999) *Biophys. J.* **77,** 2638–2642.
12. Thompson, N. L., Lieto, A. M. & Allen, N. W. (2002) *Curr. Opin. Struct. Biol.* **12,** 634–641.
13. Hope, M. J., Bally, M. B., Webb, G. & Gullis, P. R. (1985) *Biochim. Biophys. Acta* **812,** 55–65.
14. Xie, A. F., Yamada, R, Gewirth, A. A. & Granick, S. (2002) *Phys. Rev. Lett.* **89,** 246103.
15. Sukhishvili, S. A. & Granick, S. (1998) *J. Chem. Phys.* **109,** 6861–6868.
16. Xie, A. F. & Granick, S. (2002) *Nat. Mater.* **1,** 129–133.
17. Eigen, M. & Rigler, R. (1994) *Proc. Natl. Acad. Sci. USA* **91,** 5740–5747.
18. Langner, M. & Hui, S. W. (1991) *Chem. Phys. Lipids* **60,** 127–132.
19. Evans, E. & Sackmann, E. (1988) *J. Fluid Mech.* **194,** 553–561.
20. Maier, B. & Rädler, J. O. (1999) *Phys. Rev. Lett.* **82,** 1911–1914.
21. Maier, B. & Rädler, J. O. (2000) *Macromolecules* **33,** 7185–7194.
22. Stone, H. A. & Ajdari, A. J. (1998) *J. Fluid Mech.* **369,** 151–173.
23. Feigenson, G. W. & Buboltz, J. T. (2001) *Biophys. J.* **80,** 2775–2788.
24. Binder, W. H., Barragan, V. & Menger, F., M. (2003) *Angew. Chem. Int. Ed.* **42,** 5802–5827.
25. Bermúdez, H., Hammer, D. A. & Discher, D. E. (2004) *Langmuir* **20,** 540–543.